Current-induced magnetic superstructures in exchange-spring devices

Current-induced magnetic superstructures in exchange-spring devices

A. M. Kadigrobov,[1,2] R. I. Shekhter,[1] and M. Jonson[1,3,4]
[1]*Department of Physics, University of Gothenburg, SE-412 96 Gothenburg, Sweden*
[2]*Theoretische Physik III, Ruhr-Universität Bochum, D-44801 Bochum, Germany*
[3]*SUPA, Institute of Photonics and Quantum Sciences, Heriot-Watt University, Edinburgh EH14 4AS, Scotland, UK*
[4]*Department of Physics, Division of Quantum Phases and Devices, Konkuk University, Seoul 143-701, Republic of Korea*
(Received 14 May 2012; revised manuscript received 5 July 2012; published 30 July 2012)

We investigate the potential to use a magnetothermoelectric instability that may be induced in a mesoscopic magnetic multilayer (F/f/F) to create and control magnetic superstructures. In the studied multilayer two strongly ferromagnetic layers (F) are coupled through a weakly ferromagnetic spacer (f) by an "exchange spring" with a temperature-dependent "spring constant" that can be varied by Joule heating caused by an electrical dc current. We show that in the current-in-plane configuration a distribution of the magnetization, which is homogeneous in the direction of the current flow, is unstable in the presence of an external magnetic field if the length L of the sample in this direction exceeds some critical value $L_c \sim 10\ \mu$m. This spatial instability results in the spontaneous formation of a moving domain of magnetization directions, the length of which can be controlled by the bias voltage in the limit $L \gg L_c$. Furthermore, we show that in such a situation the current-voltage characteristic has a plateau with hysteresis loops at its ends and demonstrate that if biased in the plateau region the studied device functions as an exponentially precise current stabilizer.

DOI: 10.1103/PhysRevB.86.014436 PACS number(s): 85.75.−d, 73.43.Qt, 73.63.−b, 85.75.Dd

I. INTRODUCTION

A useful tool for manipulating the local magnetic order in artificially structured materials is provided by the possibility to control the magnetization of a nanomagnet by injecting an electrical current. Several such scenarios have been discussed, including the so-called spin torque transfer (STT) technique based on the suggestion by Slonczewski[1] and Berger[2] to use an injection current of spin-polarized electrons. The high current densities needed in this case can easily be achieved in electrical point contacts of submicron size, where densities of the order 10^8–10^{10} A/cm^2 can be reached without significant heating of the material,[3,4] but for larger contacts thermal heating cannot be avoided. Instead, Joule heating caused by an (unpolarized) current can be used for thermal manipulation of magnetization. In Refs. 5 and 6, this approach was proposed for varying the strength of the exchange coupling of two strongly ferromagnetic layers (F) separated by a weakly ferromagnetic spacer (f). In Ref. 6, the ability of an external magnetic field to change the relative orientation of the magnetization in the outer layers of an F/f/F trilayer magnetic stack was demonstrated. The result was that by varying the temperature, and hence varying the strength of the exchange-spring coupling through the spacer layer f, the relative orientation of the magnetization of the outer F layers could be continuously and reversibly changed from being parallel to being antiparallel. Consequently, Joule heating by forcing a dc current through the structure allows an electrothermal manipulation of the relative magnetization directions.

This kind of dc-current-induced manipulation of the magnetization direction was further studied and observed in stacks predicted to have nonlinear N- and S-shaped current-voltage characteristics (CVCs) in Refs. 6 and 7, where temporal oscillations of the magnetization direction, temperature, and electric current in the magnetic stack were also investigated.

In this work we explore the possibility to use Joule heating by a current-in-plane (CIP) dc electrical current to control the spatial distribution of the magnetization directions in an exchange-spring layered structure of the type[8] sketched in Fig. 1. We will show that if the voltage bias exceeds a critical value for which the sign of the differential resistance becomes negative, two coupled magnetic domain walls can spontaneously appear along the current flow (see Fig. 6) at a distance from each other that can be controlled by the bias voltage.

Domain formation is of course not a new phenomenon. The Gunn effect,[9] well known from the physics of semiconductors, is the name given to the spontaneous formation of (moving) electric domains in a semiconductor biased in a region of negative differential resistance (which requires N-shaped CVCs). Electric domains in normal metals can also appear (for a review see, e.g., Ref. 10). These domains differ from those in semiconductors not only by the geneses of the N-shaped current-voltage characteristics but also in that the electric instability in a metal takes place under the local electric neutrality condition. Domains in metals may be due to structural[11] and magnetic[12,13] transitions, a sharp temperature dependence of the resistance at low temperatures, and magnetic breakdown,[14–20] evaporation,[21] and melting.[22] In all these cases, however, the domain sizes are macroscopically large, typically several cm. In contrast, we will show here that the N- and S-shaped CVCs of the magnetic exchange-spring structures suggested in Refs. 5–7 may give rise to magnetothermoelectric domains with a characteristic size of the order of 10 μm. The spatial distribution of the magnetization in these stacks can vary from one corresponding to a single magnetic domain wall to a spatially periodic magnetization distribution.

The structure of the paper is as follows. In Sec. II we briefly discuss some important features of the temperature dependence of the magnetization orientation in the exchange-coupled stack sketched in Fig. 1 and derive the N-shaped CVCs that are the prerequisite for the magnetothermoelectric

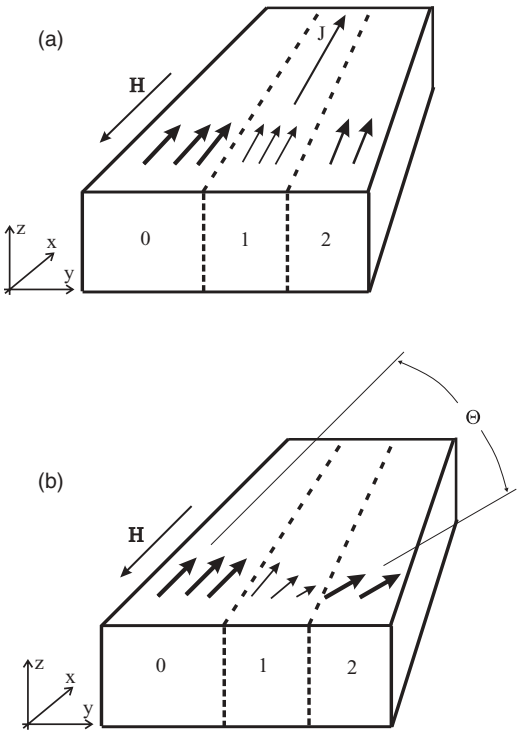

FIG. 1. Orientation of the magnetic moments in the stack of three ferromagnetic layers discussed in the text. The magnetic moments in layers 0, 1, and 2 (whose relative magnitudes are indicated by the thickness of the short arrows) are coupled by the exchange interaction thus forming an exchange spring trilayer. An external magnetic field H is directed antiparallel to the magnetization in layer 0 and a current J flows in the plane of the layers (along the x axis). In panel A the stack temperature T is lower than the critical temperature $T_c^{(\mathrm{or})}$ for the orientational phase transition in layer 1 and hence all the magnetic moments in the stack are parallel. In panel B, where $T_c^{(1)} > T > T_c^{(\mathrm{or})}$, the magnetic moments of layers 1 and 2 tilt towards the direction of the magnetic field; the angle Θ between the magnetization directions in layers 0 and 2 increases with an increase of the stack temperature T, approaching $\Theta = \pi$ as $T \to T_c^{(1)}$.

instability discussed in Sec. III. There we show that under certain conditions an instability leads to spatially highly inhomogeneous distributions of the magnetization direction in one of the layers (layer 2 in Fig. 1), of the temperature, and of the electric field inside the magnetic stack, corresponding to the formation of a stable magnetothermoelectric domain (MTED) structure in the stack. In the concluding Sec. IV we summarize the main results of the paper and estimate the values of the relevant parameters that lead to MTED formation.

II. N-SHAPED CURRENT-VOLTAGE CHARACTERISTICS OF A MAGNETIC STACK UNDER JOULE HEATING

The magnetic stack under consideration has three ferromagnetic layers as shown in Fig. 1. The outer two layers (0 and 2) are strongly ferromagnetic and coupled via the exchange interaction through a weakly ferromagnetic spacer layer (1). The Curie temperature $T_c^{(1)}$ of layer 1 is assumed to be lower than the Curie temperatures $T_c^{(0,2)}$ of layers 0 and 2. In addition we assume the magnetization direction of layer 0 to be fixed. A static external magnetic field H, directed opposite to the magnetization of layer 0, is required to be weak enough that at low temperatures T the magnetization of layer 2 is kept parallel to the magnetization of layer 0 due to the exchange interaction between them via layer 1. At $H = 0$ and $T > T_c^{(1)}$ this trilayer is similar to the spin-flip "free layer" widely used in memory device applications.[23] The stack is incorporated into an external circuit in such a way that a current J flows through the cross-section of the layers and

$$J = \left[\frac{1}{R(\Theta)} + \frac{1}{R_0}\right] V . \tag{1}$$

Here $R(\Theta)$ and R_0 are the magnetoresistance and the angle-independent resistance of the stack, Θ is the angle between the magnetization directions of layers 0 and 2, and V is the voltage drop across the stack.

In Ref. 6 it was shown that a magnetic configuration with parallel orientations of the magnetization in layers 0, 1, and 2 becomes unstable if the temperature exceeds some critical temperature $T_c^{(\mathrm{or})} < T_c^{(1)}$. The magnetization direction in layer 2 smoothly tilts with an increase of the stack temperature T in the temperature interval $T_c^{(\mathrm{or})} \leqslant T \leqslant T_c^{(1)}$ (see Fig. 1). The dependence of the equilibrium tilt angle Θ between the magnetization directions of layers 0 and 2 on T and the magnetic field H is determined by the equation[6]

$$\begin{aligned} &\Theta = D(H,T)\sin\Theta, \quad T < T_c^{(1)}, \\ &\Theta = \pm\pi, \quad T \geqslant T_c^{(1)}, \end{aligned} \tag{2}$$

where

$$D(H,T) = \frac{L_1 L_2 H M_2(T)}{4\alpha_1 M_1^2(T)} \approx D_0(H)\frac{T_c^{(1)}}{T_c^{(1)} - T} \tag{3}$$

and

$$D_0(H) = \frac{\mu_B H}{k_B T_c^{(1)}}\left(\frac{L_1}{a}\right)\left(\frac{L_2}{a}\right). \tag{4}$$

Here $L_{1,2}$ and $M_{1,2}(T)$ are the widths and the magnetic moments of layers 1 and 2, respectively; $\alpha_1 \sim I_1/aM_1^2(0)$ is the exchange constant, I_1 is the exchange energy in layer 1, μ_B is the Bohr magneton, k_B is Boltzmann's constant, and a is the lattice spacing. $D(H,T)$ is a dimensionless parameter that determines how effective the external magnetic field is to cause the misorientation effect under consideration. More precisely, it is the ratio between the energy of magnetic layer 2 in the external magnetic field and the energy of the indirect exchange between layers 0 and 2 (see Fig. 2). At low temperatures the indirect exchange energy prevails, the parameter $D(H,T) < 1$, and Eq. (2) has only one root, $\Theta = 0$; thus a parallel orientation of magnetic moments in layers 0, 1, and 2 of the stack is thermodynamically stable. However, at temperature $T_c^{(\mathrm{or})} < T_c^{(1)}$, for which

$$D\left(T_c^{(\mathrm{or})}, H\right) = 1,$$

two new solutions, $\Theta = \pm|\theta_{\min}| \neq 0$, appear. The parallel magnetization corresponding to $\Theta = 0$ is now unstable, and the direction of the magnetization in region 2 tilts with an increase of temperature in the interval $T_c^{(\mathrm{or})} \leqslant T \leqslant T_c^{(1)}$ [see Fig. 1(b)]. The critical temperature $T_c^{(\mathrm{or})}$ of this orientational

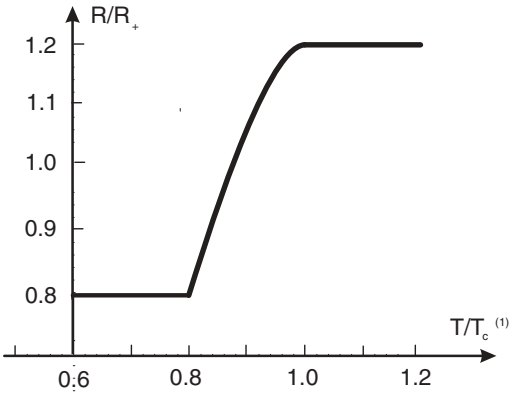

FIG. 2. Normalized temperature dependence of the magnetic stack resistance, $R = R[\Theta(T)]$, as determined by the T dependence according to Eq. (2) of the angle $\Theta(T)$ between the magnetization directions in layers 0 and 2 of Fig. 1. The calculations were made for $R_-/R_+ = 0.2$, $D_0 = 0.2$; $R_\pm = R(\pi) \pm R(0)$ and $T_c^{(1)}$ is the Curie temperature of the spacer layer 1 between layers 0 and 2.

phase transition is obtained from Eq. (3) as[24]

$$T_c^{(\mathrm{or})} = T_c^{(1)}\left(1 - \frac{\delta T}{T_c^{(1)}}\right), \quad \frac{\delta T}{T_c^{(1)}} = D_0(H). \tag{5}$$

The orientational transition discussed above can be detected by measuring the temperature dependence of the stack magnetoresistance,[26] $R = R[\Theta(T)]$, plotted for a typical case in Fig. 2. This temperature dependence is caused by the temperature dependence of the misalignment angle $\Theta = \Theta(T)$, which is implicitly given by Eq. (2).

If the stack is Joule heated by a current J its temperature $T(V)$ is determined by the heat-balance condition

$$JV = Q(T), \quad J = V/R_{\mathrm{eff}}(\Theta), \tag{6}$$

where

$$R_{\mathrm{eff}}(\Theta) = \frac{R(\Theta)R_0}{R(\Theta) + R_0}, \tag{7}$$

in conjunction with Eq. (2), which determines the temperature dependence of Θ. Here V is the voltage drop across the stack, $Q(T)$ is the heat flux flowing from the stack, and $R_{\mathrm{eff}}(\Theta)$ is the total stack magnetoresistance. Here and below we neglect the explicit dependence of the magnetoresistance on T since we consider a thin stack in which elastic scattering of electrons is the main mechanism of the stack resistance. On the other hand, we consider the temperature changes caused by the Joule heating only in a narrow vicinity of $T_c^{(1)}$, which is sufficiently lower than both the critical temperatures $T_c^{(0,2)}$ and the Debye temperature.

Equations (2) and (6) define the CVCs of the stack,

$$J(V) = \frac{V}{R_{\mathrm{eff}}\,[\Theta(V)]}, \tag{8}$$

where $\Theta(V) \equiv \Theta[T(V)]$. Below we will simplify the notation by dropping the subscript "eff" and simply write $R(\Theta)$.

The dependencies of the tilt angle Θ on temperature T and of the resistance R on the tilt angle Θ can result in a negative differential resistance. This can be qualitatively understood by noting that if $T < T_c^{(\mathrm{or})}$ there is no tilt, $\Theta = 0$, and an

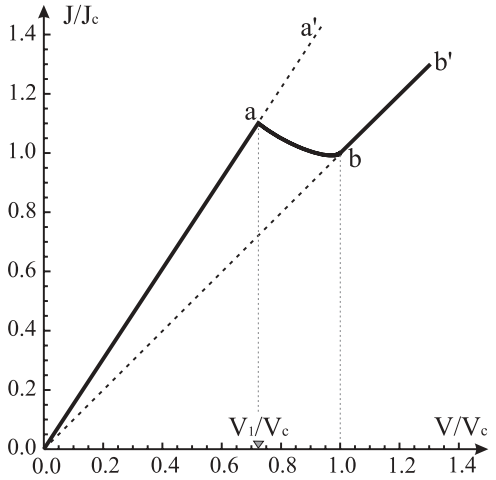

FIG. 3. Current-voltage characteristics (CVCs) of the magnetic stack of Fig. 1 in which the magnetization directions in the layers are homogeneously distributed along the x direction (along the stack). They were calculated for $R(\Theta) = R_+ - R_- \cos\Theta$, $R_-/R_+ = 0.2$, $D_0 = 0.2$; $J_c = V_c/R(\pi)$; $V_c = \sqrt{R(\pi)Q(T_c^{(1)})/\Omega_{\mathrm{st}}}$. The branches 0-$a$ and b-b' of the CVCs correspond to parallel and antiparallel orientations of the stack magnetization, respectively (the parts a-a' and 0-b are unstable); the branch a-b corresponds to $0 \leqslant \Theta[T(V)] \leqslant \pi$.

increase of the applied voltage V increases the current J [see Eq. (8)] without changing the stack resistance, $R = R(0)$. This corresponds to the CVC branch $0 - a$ in Fig. 3. With a further increase of V, Joule heating increases the temperature above $T_c^{(\mathrm{or})}$ so that the tilt angle starts to increase. This leads to an increase of the resistance (see Fig. 2), which *may* decrease the current with a further increase of V as is shown in Fig. 3. Below we find the range of parameters for which the differential resistance *does* become negative.

Differentiating both equations in Eq. (6) with respect to V one finds (see Appendix A)

$$\frac{dJ(V)}{dV} = R\,[\Theta(T)]\,\frac{d(R^{-1}\,[\Theta(T)]\,Q(T))/dT}{d(R\,[\Theta(T)]\,Q(T))/dT}\bigg|_{T=T(V)}.$$

From here it is clear that the differential conductance of the stack, dJ/dV, is negative if the sample is Joule heated to a temperature at which

$$d\{Q(T)/R[\Theta(T)]\}/dT < 0.$$

Therefore, the main properties of the system under consideration are determined by the behavior of the function $\chi = Q(T)/R[\Theta(T)]$ plotted for typical parameters in the top panel of Fig. 4.

In the same manner, using Eq. (2) one may express the differential conductance in terms of the dependence of the magnetoresistance R on the magnetization angle Θ as[6]

$$\frac{dJ}{dV} = R\,(\Theta)\,\frac{[R^{-1}(\Theta)(1 - \bar{D}\sin\Theta/\Theta)]'}{[R(\Theta)(1 - \bar{D}\sin\Theta/\Theta)]'}\bigg|_{\Theta=\Theta(V)}, \tag{9}$$

where $[\ldots]'$ means the derivative of the bracketed quantity with respect to Θ, and

$$\bar{D} = \frac{T}{Q}\frac{dQ}{dT}D_0\bigg|_{T=T_c^{(1)}} \approx D_0.$$

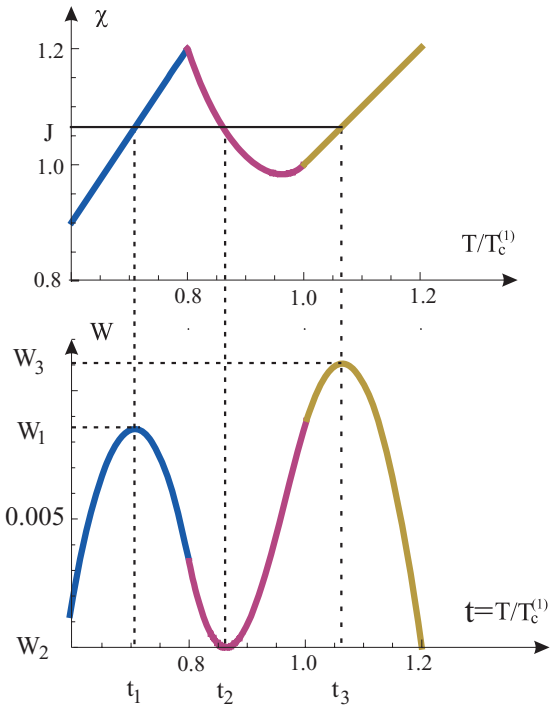

FIG. 4. (Color online) Plots of the function $\chi(T) = Q(T)/R[\Theta(T)]$ and the "potential" energy $W(T,J)$ calculated for $R(\Theta) = R_+ - R_- \cos\Theta$, $R_-/R_+ = 0.2$, $D_0 = 0.2$, and $J/J_c = 1.03$; $J_c = V_c/R(\pi)$; $t_{1,2,3} = T_{1,2,3}/T_c^{(1)}$.

It follows from Eq. (9) that the differential conductance dJ/dV is negative if

$$\frac{d}{d\Theta}\frac{(1-\bar{D}\sin\Theta/\Theta)}{R(\Theta)} < 0. \tag{10}$$

In this case the current-voltage characteristics (CVCs) of the stack are N-shaped as shown in Fig. 3.

Using Eqs. (1) and (9) and assuming the magnetoresistance to be of the form[27] $R(\Theta) = R_+(1 - r\cos\Theta)$, where

$$r = \frac{R_-}{R_+} > 0, \qquad R_\pm = \frac{R(\pi) \pm R(0)}{2}, \tag{11}$$

one finds that the differential conductance dJ/dV is negative if

$$\bar{D} < \frac{3r[R(0) - (1-r)^2 R_+]}{(1+2r)R(0) + (1-r)^2(1-4r)R_+}. \tag{12}$$

It follows that CVCs with a negative differential resistance are possible if $R(0) > (1-r)^2 R_+$.

In the case that the stack has a negative differential resistance, nonlinear current and magnetization-direction oscillations may spontaneously arise if the stack is incorporated in a voltage-biased electrical circuit in series with an inductor.[6,7] In this paper we show that another type of magnetoelectrical instability can arise in such a stack if the electrical current flows in the plane of the layers (CIP configuration): A homogeneous distribution of magnetization direction, temperature, and electric field along the spring-type magnetic stack becomes unstable and a magnetothermoelectric domain spontaneously arises in the stack. Here and below we consider the case that the electrical current flowing through the sample is lower than the torque critical current and hence the torque effect is absent.[28]

III. MAGNETOELECTROTHERMAL INSTABILITY IN A MAGNETIC STACK

In this section we will work in the voltage bias regime, where the resistance of the external circuit into which the magnetic stack is incorporated can be neglected in comparison with that of the stack. In this case, using the known relation between the electric field and the temperature (see, e.g., Ref. 30) and taking into account that the temperature, $T(x,t)$, being a function of the coordinate x along the stack and time t, satisfies the continuity equation for the heat flow, one obtains a set of basic equations for the problem,

$$\begin{aligned} &c_v\frac{\partial T}{\partial t} + j(t)T\frac{d\alpha}{dT}\frac{\partial T}{\partial x} - \frac{\partial}{\partial x}\left(\kappa(T)\frac{\partial T}{\partial x}\right) = -f(T,j), \\ &f(T,j) = Q(T)/\Omega_{\rm st} - j^2(t)\rho[\theta(T)], \\ &j(t)\langle\rho\rangle = \frac{V}{L}, \end{aligned} \tag{13}$$

where the T-dependence of $\Theta(T)$ is given by Eq. (2). Furthermore, $j(t) = J(t)/S$ is the current density, which is independent of x due to the condition of local electrical neutrality, S is the cross-section area of the stack and L is its length, c_v is the heat capacity per unit volume, α is the proportionality coefficient between the electric field and the temperature gradient,[30] κ is the thermal conductivity, $Q(T)$ is the heat flux flowing from the stack, $\Omega_{\rm st}$ is its volume, and $\rho[\theta] = R_{\rm eff}[\theta]S/L$ is the stack magnetoresistivity [see Eq. (7)]; the brackets $\langle\cdots\rangle$ that appear in the last part of Eq. (13) indicate an average over x along the whole stack of length L.

The boundary condition needed to solve Eq. (13) is the continuity of the heat flux at both ends of the stack (which is coupled to an external circuit with a fixed voltage drop V over the stack). We shall not write down any explicit expression for this condition, since it will become clear below that the magnetothermal domain structure does not depend on the boundary conditions if L is sufficiently large. Instead, we use the periodic boundary condition[31] $T(x+L,t) = T(x,t)$.

The set of equations (13) always has the steady-state homogeneous solution

$$\begin{aligned} &T = T_0(V), \quad \Theta = \Theta_0(V) \equiv \Theta[T_0(V)], \\ &j_0 = \rho^{-1}[\Theta(T_0)]V/L, \quad f(T_0, j_0) = 0. \end{aligned} \tag{14}$$

The last equation in Eq. (14) is identical to the energy balance condition (6) which, together with Eq. (2), determines the N-shaped CVCs shown in Fig. 3.

As shown in Appendix B, if the differential conductance dJ/dV is negative the uniform magnetization along the stack is stable only if the stack length L is shorter than some critical length L_c, where

$$L_c = \sqrt{\frac{2\pi\kappa\overline{D}T_c^{(1)}}{j_c^2\rho(\pi)}\frac{\rho^{-1}(\Theta_0)(\sin\Theta/\Theta)'}{[\rho^{-1}(\Theta)(1-\overline{D}\sin\Theta/\Theta)]'}} \tag{15}$$

and the derivatives with respect to Θ are evaluated for $\Theta = \Theta_0$. However, when $L > L_c$ the uniform distribution of

the stack magnetization becomes unstable against fluctuations comprising an arbitrary sum of harmonics $A_n \exp(i2\pi nx/L)$ $(n = \pm 1, \pm 2 \ldots)$ with $|n| < L/L_c$. A fluctuation with $|n| > L/L_c$ or $|n = 0|$ (uniform fluctuation), on the other hand, does not destroy the stability of the homogeneous solution (14) [see Eq. (B2)]. We note here that the characteristic value of the critical length can be rather short. Using Eqs. (9) and (15) and the Lorentz ratio $\kappa/\sigma = \pi^2 k_B^2 T/3e$, where $\sigma = 1/\rho$ and e is the electron charge, one finds that

$$L_c \sim \sqrt{\frac{\kappa}{r}\frac{T_c^{(1)}}{\rho(0) j_c^2}} \sim \frac{\pi}{\sqrt{r}}\frac{k_B T_c^{(1)}}{e\rho(0) j_c} \sim 10\ \mu\text{m} \qquad (16)$$

for a realistic experimental situation: $r \sim 0.1$–0.3, $T_c^{(1)} \sim 100$ K, $\rho(0) \sim 10\ \mu\Omega$cm, $j \sim 10^6$–10^7 A/cm^2.

Therefore, in the range of parameters $L > L_c$ homogeneous distributions of the magnetization direction Θ, temperature

$$T = T_c^{(1)}\left(1 - D_0 \frac{\sin\Theta}{\Theta}\right) \qquad (17)$$

[see Eqs. (2) and (3)], and the electric field

$$\mathcal{E} = \rho[\Theta(T)] j \qquad (18)$$

along the system are unstable, and a magnetothermoelectric domain, moving with a constant velocity s, may spontaneously arise inside the magnetic stack:[32]

$$\begin{aligned} &T(x,t) = \nu(x - st, j_d), \quad j_d(V) = \frac{V}{L}\langle\rho[\Theta_d]\rangle^{-1}, \\ &\Theta(x,t) = \Theta_d(x - st) \equiv \Theta[\nu(x - st, j_d)], \end{aligned} \qquad (19)$$

where the definition of the brackets $\langle \cdots \rangle$ is the same as in Eq. (13), and $\nu(x)$ satisfies the equation of motion of a fictitious particle of variable "mass" $\kappa(\nu)$ governed by a potential force $f(\nu, j)$ and a friction force proportional to $d\nu/dx$:

$$\frac{d}{dx}\left(\kappa(\nu)\frac{d\nu}{dx}\right) + \left(c_v s - j_d \nu \frac{d\alpha}{d\nu}\right)\frac{d\nu}{dx} = f(\nu, j_d) \qquad (20)$$

(here x is the "time" and ν is the "coordinate" of the particle).

The velocity s of the domain is found from the condition that the total change of energy $E(x)$ in the "period" L vanishes [that is, $\delta E = 0$; see Eq. (C5)]:

$$s = j\left\langle \kappa(\nu)\nu\frac{d\alpha}{d\nu}\left(\frac{d\nu}{dx}\right)^2\right\rangle \Big/ \left\langle \kappa(\nu) c_v(\nu)\left(\frac{d\nu}{dx}\right)^2\right\rangle. \qquad (21)$$

Hence, the velocity of a magnetothermoelectric domain is

$$s \sim j\alpha/c_v \sim j\frac{1}{c_v T_c^{(1)}}\frac{k_B T_c^{(1)}}{e}\frac{k_B T_c^{(1)}}{\varepsilon_F} \sim 10\ \text{cm/s}$$

for $j \sim 10^6$–10^7 A/cm^2, $c_v \sim 1$ J/K cm^3, $T_c^{(1)} \sim 100$ K.

In the same manner as for Gunn domains in semiconductors[9] and electric domains in superconductors and normal metals,[10] the motion of the MTED domain can be stopped by inhomogeneities inside the stack or at its ends. As the MTED velocity is low, even weak inhomogeneities can pin the MTED. However, in very homogeneous samples there is a possibility that thermal domains can move along the sample, periodically disappearing at one end of the sample and then reappearing at the other, so that the result is temporal nonlinear electrical oscillations[34] with period $\omega \sim L/s$. In the case under consideration these oscillations involve the magnetization direction Θ, temperature T, and electrical current j. Using the parameter values already introduced one gets $\omega = s/L \sim 1$–10 MHz for a magnetic stack of length $L \sim 1\ \mu$m.

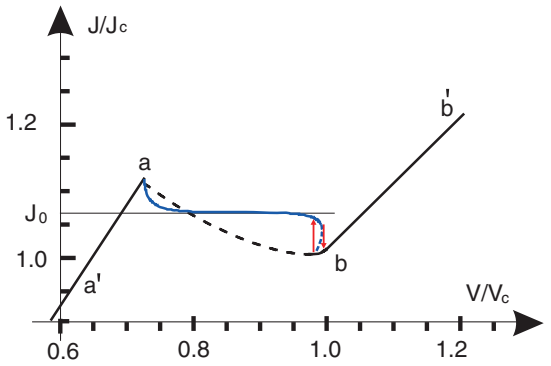

FIG. 5. (Color online) Current-voltage characteristics (CVCs) of the magnetic stack of Fig. 1 for $L \gg L_c$, i.e., when the stack contains a magnetothermoelectric domain. The CVCs were calculated for $R(\Theta) = R_+ - R_- \cos\Theta$, $R_-/R_+ = 0.2$, $D_0 = 0.2$; $J_c = V_c/R(\pi)$; $V_c = \sqrt{R(\pi)Q(T_c^{(1)})/\Omega_{\text{st}}}$. The branches a'-a and b-b' of the CVCs correspond to parallel and antiparallel orientations of the stack magnetization, respectively, while the solid branch a-b corresponds to a stable magnetothermoelectric domain (MTED) spontaneously formed inside the stack. The dashed lines indicate sections where the CVCs are unstable. The red vertical arrows indicate the hysteresis loop in the CVCs caused by the disappearance and emergence of the MTED as the bias voltage is changed. The thin horizontal line shows the stabilization current J_0.

As shown in Appendix C [see Eqs. (C6) and (C7)], the function $\nu(x)$ satisfies the following equation with a high accuracy:

$$\frac{1}{2}\left(\kappa\frac{d\nu}{dx}\right)^2 + W(\nu, j_d) = E. \qquad (22)$$

In this approximation the domain velocity is determined by the equation

$$\begin{aligned} s = j_d &\int_{T_{\min}}^{T_{\max}} T\frac{d\alpha}{dT}\sqrt{E - W(T, j_d)}\,dT \\ &\Big/ \int_{T_{\min}}^{T_{\max}} c_V(T)\sqrt{E - W(T, j_d)}\,dT, \end{aligned} \qquad (23)$$

where $T_{\min}$ and $T_{\max}$ are the minimal and maximal temperatures in the domain obtained as real roots of the equation $W(T, j) = E$. Here the constant E plays the role of "particle" energy, which determines the "period of motion," $\widetilde{L}(E, j)$, of a nonlinear oscillator. Its value is found from the condition that $\widetilde{L}(E, j)$ is equal to the length L of the magnetic stack; that is, the magnetothermoelectric domain $\nu(x)$ as a function of x has only one maximum and one minimum along the length of the magnetic stack. In the case $\widetilde{L}(E, j) = L/n$ (where $n = 2, 3, \ldots$), "multiple" domains are also possible.

The solution of Eq. (22), together with Eq. (17), defines the spatial distributions of temperature and magnetization direction in a magnetic stack with a magnetothermoelectric

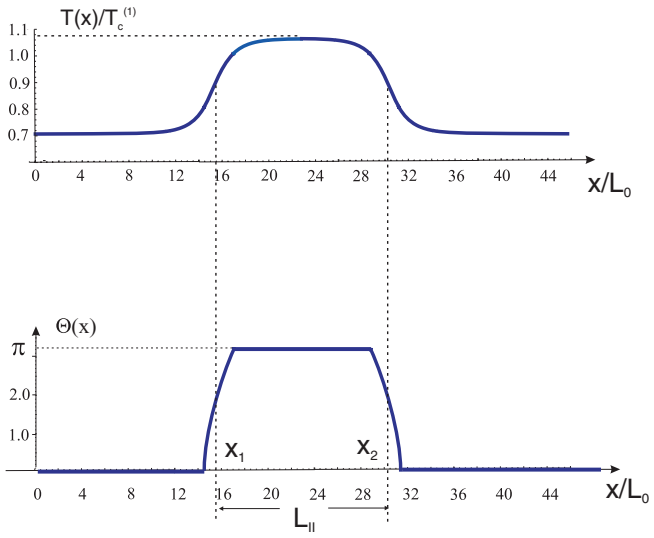

FIG. 6. (Color online) Coordinate dependence of the temperature, $T(x)$, and the magnetization-misorientation angle, $\Theta(x)$, in a magnetic stack containing a magnetothermoelectric domain, calculated for $R(\Theta) = R_+ - R_- \cos\Theta$, $R_-/R_+ = 0.2$, $D_0 = 0.2$; $J/J_c = 1.0265$, $J_c = V_c/R(\pi)$, $V_c = \sqrt{R(\pi)Q(T_c^{(1)})/\Omega_{\rm st}}$, $L_0 = [j_c^2\rho(\pi)/\kappa T_c^{(1)}]^{(1/2)} \sim L_c$.

domain. Typical examples of such distributions are presented in Fig. 6.

Using Eq. (22) and the last equation in (19) one finds the set of equations

$$\widetilde{L}(E,j) \equiv \sqrt{2}\int_{\nu_{\min}(j)}^{\nu_{\max}(j)} \frac{\sqrt{\kappa}\,dT}{\sqrt{E - W(T,j)}} = L, \qquad (24)$$

$$j\sqrt{2}\int_{\nu_{\min}(j)}^{\nu_{\max}(j)} \rho(\Theta(T))\frac{\sqrt{\kappa}\,dT}{\sqrt{E - W(T,j)}} = V. \qquad (25)$$

The solutions $E = E_d(V,L)$ and $j = j_d(V,L)$ of these equations are, respectively, the "energy" of the domain and the current-voltage characteristics of the magnetic stack containing a magnetothermoelectric domain (the dynamic CVCs). In Eqs. (24) and (25) the limits of integration, $\nu_{\min}$ and $\nu_{\max}$, i.e., the minimum and maximum temperature of the domain, are obtained as the real roots of the equation $W(\nu, j) = E$.

Let us consider the most pronounced case, for which $L \gg L_c$. In this limit we find a solution of Eq. (22) that has a period much larger than L_c. Since the period $\widetilde{L}(E,j)$ of the nonlinear oscillator [see Eq. (24)] diverges logarithmically as $E \to \min\{W_{1,3}(j)\}$ [where $W_{1,3}(j)$ are the maxima of the "potential" energy; see Fig. 4], this condition is satisfied if the "energy" $E = E(L,j)$ of the domain differs from $\min\{W_1, W_3\}$ by an exponentially small amount. From here it follows that variations of the current inside a narrow interval around j_0, defined by the relation

$$\int_{T_1(j_0)}^{T_3(j_0)} \kappa(T) f(T, j_0) dT = 0,$$

drastically changes the form of the magnetothermoelectric domain and hence the current voltage characteristics. Solving the set of equations (24) and (25) in the interval $|j - j_0| \ll j_0$ [where $W_1(j) \approx W_3(j) \approx W(j_0)$] and taking into account that the maximal, $\nu_{\max}$, and minimal, $\nu_{\min}$, temperatures of the domain are close to T_1 and T_3, respectively, one finds the following implicit form of the dynamic CVCs:

$$j - j_0 = J_I \exp\left\{-\frac{\bar{\mathcal{E}} - \rho(0)j}{r(j_0\rho_+)}\frac{L}{L_0}\right\} - J_{II}\exp\left\{\frac{\bar{\mathcal{E}} - \rho(\pi)j}{r(j_0\rho_+)}\frac{L}{L_0}\right\}. \qquad (26)$$

Here $\bar{\mathcal{E}} = V/L$, $L_0 = [f_T'(T_c^{(1)})/\kappa]^{(1/2)} \sim L_c$, and the constants $J_{I,II}$ are of the order of j_0 while $f'_T = \partial f/\partial T$.

Differentiating both sides of Eq. (26) with respect to $\bar{\mathcal{E}}$ one finds that the dynamic CVCs have vertical tangents at the two points $(J_1, \bar{\mathcal{E}}_1)$ and $(j_2, \bar{\mathcal{E}}_2)$, where

$$j_1 = j_0(1 + \lambda(0)), \quad \bar{\mathcal{E}}_1 = \rho(0)j_0\{1 + \lambda(0)[1 - \ln\lambda(0)]\} \qquad (27)$$

and

$$j_2 = j_0(1 + \lambda(\pi))\bar{\mathcal{E}}_2 = \rho(\pi)j_0\{1 - \lambda(\pi)[1 - \ln\lambda(\pi)]\} \qquad (28)$$

while

$$\lambda(\Theta) = \frac{L_0}{L}\frac{\rho(\pi) - \rho(0)}{\rho(\Theta)}. \qquad (29)$$

It follows from the above equations that the values of the currents j_1 and j_2 differ from j_0 by an amount $\sim j_0(L_c/L)$.

One can see from Eq. (26) and Eq. (29) that for all values of $\bar{\mathcal{E}} = V/L$ in the interval $\bar{\mathcal{E}}_1 < \bar{\mathcal{E}} < \bar{\mathcal{E}}_2$, except for a small region near the ends of the interval, the current j coincides with j_0 to an accuracy that is exponential in the parameter $L/L_c \gg 1$. A change of the bias voltage in this interval does not change the current but it does change the length of the magnetothermoelectric domain, that is the length of the higher resistive part of it providing the needed voltage drop across the stack at the fixed current value $J = J_0$. Therefore, a magnetic stack with a magnetothermoelectric domain inside can work as a high-quality current stabilizer.

Near the points $\bar{\mathcal{E}}_1$ and $\bar{\mathcal{E}}_2$ there is a sharp transition from the nearly horizontal segment of the dynamic CVCs to the rising segments of the CVCs corresponding to a homogeneous state of the magnetic stack (see Fig. 5). As a result, there are hysteresis loops in the current-voltage characteristics of the stack of a large enough length L.

The fact, mentioned above, that the current is nearly independent of the bias voltage in the interval $[V_1, V_2]$ (here $V_{1,2} = L\mathcal{E}_{1,2}$) comes about because in this region the domain structure can be written to exponential accuracy [i.e., with an error $\propto \exp(-L/L_c)$] as

$$T_d(x) = \vartheta(x + x_1) + \vartheta(x_2 - x) - T_{\max}, \qquad (30)$$

where the function $\vartheta(x)$ is a domain-wall-type solution of Eq. (20) at $j = j_0$ and $L \to \infty$, the asymptotic behavior of which is

$$\lim_{x\to-\infty} = \vartheta(x) \to T_{\min}, \quad \lim_{x\to\infty} = \vartheta(x) \to T_{\max}. \qquad (31)$$

Here $x_{1,2}$ are the points of deflections of the curve $dT_d(x)/dx$ so that $L_{II} = x_2 - x_1$ is approximately the length of the "hot" section of a trapezoidal MTED having the maximal

temperature $T_{\max}$ and $L_I = L - L_{II}$ is the length of its "cold" section having the minimal temperature $T_{\min}$ (see Fig. 6).

IV. CONCLUSION

We have shown that Joule heating of the magnetic stack sketched in Fig. 1 by a current flowing in the plane of the layers may result in an instability of an initially homogeneous distribution of the magnetization of the stack if the length L of the stack in the direction of the current flow is longer than some critical length L_c. This instability results in the spontaneous appearance of moving domains of magnetization direction in layer 2 of Fig. 1, $\Theta(x - \mathrm{st})$, temperature, $T(x - \mathrm{st})$, and electric field, $\mathcal{E}(x - \mathrm{st})$. For the case $L \gtrsim L_c$ the length of the domain is of the order of L_c.

If the length of the stack greatly exceeds the critical length, $L \gg L_c$, the stack is spontaneously divided into two regions, where in one region the magnetization directions in layer 1 and layer 2 of Fig. 1 are parallel to each other, while in the other region they are antiparallel. The length of the region with antiparallel magnetization orientations (that is the length of the domain L_d) is controlled by the bias voltage in the interval $L_c \lesssim L_d \lesssim L$ (see Fig. 6). In this case the CVCs of a stack containing such a domain have a plateau with hysteresis loops at the ends, as shown in Fig. 5. Therefore, the stack can work as a current stabilizer since the current flowing through it has a fixed value J_0 to within an exponentially small error $\propto \exp(-L/L_c)$; a change of bias voltage only results in a change of the domain length to provide the needed voltage drop over the stack.

For a realistic experimental situation the value of the parameter r, which through Eq. (11) determines the dependence of the stack resistance on the magnetization-misorientation angle Θ, can be estimated to be of order 0.1–0.3, while the Curie temperature $T_c^{(1)}$ of the spacer layer 1 can be $\sim$100 K. Using these values and a resistivity of $\rho(\Theta = 0) \sim 10\,\mu\Omega\,\mathrm{cm}$, a current density of $j \sim 10^6$–10^7 A/cm^2, and a specific heat of $c_v \sim 1$ J/K cm^3, one finds that the critical length is $L_c \sim 10\ \mu$m.

ACKNOWLEDGMENTS

Financial support from the European Commission (FP7-ICT-FET Project No. 225955 STELE), the Swedish VR, and the Korean WCU program funded by MEST/NFR (R31-2008-000-10057-0) is gratefully acknowledged.

APPENDIX A: NEGATIVE DIFFERENTIAL CONDUCTANCE

Inserting $R(T) \equiv R(\Theta(T))$ in Eq. (6) one gets

$$J = \frac{V}{R(T)}, \quad V^2 = Q(T)R(T). \tag{A1}$$

Differentiating the both equations with respect to V one finds

$$\frac{dJ}{dV} = \left[\frac{1}{R} - \frac{R_T'}{R^2} V \frac{dT}{dV}\right]_{T=T(V)}, \quad V\frac{dT}{dV} = \left[\frac{2QR}{(QR)_T'}\right]_{T=T(V)}, \tag{A2}$$

where $f_T' \equiv df/dT$ and $T(V)$ is determined by the second equation in Eq. (A1). From here one readily obtains

$$\frac{dJ}{dV} = \frac{1}{R}\frac{RQ_T' - R_T'Q}{(RQ)_T'}\bigg|_{T=T(V)} = R\frac{(R^{-1}Q)_T'}{(RQ)_T'}\bigg|_{T=T(V)}. \tag{A3}$$

APPENDIX B: INSTABILITY OF A MAGNETIZATION DISTRIBUTION THAT IS SPATIALLY HOMOGENEOUS IN THE PLANE OF THE MAGNETIC LAYERS

In order to investigate the stability of the spatially homogeneous solution (14) for temperature, $T = T_0$, current density, $j = j_0$, and magnetization-misalignment angle, $\Theta = \Theta_0$, against spatial fluctuations we express these quantities as sums of two terms,

$$\begin{aligned} T &= T_0(V) + T_1(x,t), \quad \Theta = \Theta_0(V) + \Theta_1(x,t), \\ j &= j_0 + j_1(t), \end{aligned} \tag{B1}$$

where T_1, Θ_1, and j_1 are each a small correction. Inserting Eq. (B1) into Eqs. (2) and (13) and using the Fourier expansion

$$\begin{aligned} T_1(t,x) &= \sum_{n=-\infty}^{+\infty} T_1^{(n)}(t)\exp\{ik_n x\}, \\ \Theta_1(t,x) &= \sum_{n=-\infty}^{+\infty} \Theta_1^{(n)}(t)\exp\{ik_n x\}, \quad k_n = \frac{2\pi n}{L}, \end{aligned}$$

one finds that

$$T_1^{(n)}(t) = D_0 T_c^{(1)} |(\sin\Theta_0/\Theta_0)'| \Theta_1^{(n)}(t),$$

while the equation for the Fourier harmonics of the angle are

$$c_v \frac{d\Theta_1^{(0)}}{dt} = -\left\{\frac{j_c^2\rho(\pi)}{D_0 T_c^{(1)}|(\sin\Theta/\Theta)'|} \times \frac{1}{\rho(\Theta)}[\rho(\Theta)(1 - \overline{D}\sin\Theta/\Theta)]'\right\}_{\Theta=\Theta_0} \Theta_1^{(0)} \tag{B2}$$

if $n = 0$, and

$$\frac{c_v}{\kappa}\frac{d\Theta_1^{(n)}}{dt} = -\left(\frac{2\pi}{L}\right)^2 n^2 - \left\{\frac{j_c^2\rho(\pi)}{\kappa D_0 T_c^{(1)}|(\sin\Theta/\Theta)'|} \times \rho(\Theta)[\rho^{-1}(\Theta)(1 - \overline{D}\sin\Theta/\Theta)]'\right\}_{\Theta=\Theta_0} \Theta_1^{(n)} \tag{B3}$$

if $n \neq 0$.

From this result one sees that if

$$[\rho^{-1}(\Theta)(1 - \overline{D}\sin\Theta/\Theta)]'_{\Theta=\Theta_0} < 0$$

[that is if $dJ/dV < 0$, see Eq. (9)] the uniform magnetization along the stack loses its stability if the stack length exceeds some critical value. Setting the right-hand side of Eq. (B3) equal to zero one gets the result (15) for the critical length L_c.

APPENDIX C: DOMAIN STRUCTURE

By multiplying both sides of Eq. (20) by $\kappa(v)\partial v/\partial x$ one gets the equation

$$\frac{d}{dx}\left[\frac{1}{2}\left(\kappa\frac{dv}{dx}\right)^2 + W(v,j_d)\right] = -\kappa^{-1}\left(c_v s - j_d v\frac{d\alpha}{dv}\right)\left(\kappa\frac{dv}{dx}\right)^2, \quad \text{(C1)}$$

where the quantity

$$E(x) = \frac{1}{2}\left(\kappa\frac{dv}{dx}\right)^2 + W(v,j_d) \quad \text{(C2)}$$

plays the role of the total "energy" of a fictitious particle, the first term giving the "kinetic energy" and the "potential energy" being defined as

$$W(T,j) = -\int_{T_2(j)}^{T}\kappa(T')f(T',j)dT' \quad \text{(C3)}$$

[the dependence of $W(T,j)$ on T is shown in Fig. 4].

The change of energy with "time" x is caused by the action of the "friction" force:

$$\frac{dE}{dx} = -\kappa^{-1}\left(c_v s - j_d v\frac{d\alpha}{dv}\right)\left(\kappa\frac{dv}{dx}\right)^2. \quad \text{(C4)}$$

Integrating this equation one finds the change of the energy $E(x)$ during the "period" L

$$\delta E = -\int_0^L \kappa^{-1}\left(c_v s - j_d v\frac{d\alpha}{dv}\right)\left(\kappa\frac{dv}{dx}\right)^2 dx. \quad \text{(C5)}$$

From here it follows that $\delta E = 0$ if the domain velocity s satisfies Eq. (21).

As one sees from Eq. (C1), the ratio of the "friction force" to the "inertial" term is of the order

$$\xi = j\frac{\alpha L_c}{\kappa} \sim \alpha\sqrt{\frac{T_c^{(1)}}{r\rho\kappa}} \sim \frac{k_B T_c^{(1)}}{\varepsilon_F\sqrt{r}} \sim 10^{-4}, \quad \text{(C6)}$$

where ε_F is the Fermi energy. From here it follows that the right-hand sides of Eqs. (C1) and (C4) are of the order of

$$\frac{1}{L_c}\frac{kT}{\varepsilon_F}\left(\kappa\frac{dv}{dx}\right)^2 \sim 10^{-4}\frac{1}{L_c}\left(\kappa\frac{dv}{dx}\right)^2 \quad \text{(C7)}$$

and hence the function $v(x)$ satisfies an "energy" conservation law $E(x) = E = \text{const}$ [see Eq. (C2)] to within an error $\sim k_B T_c^{(1)}/\varepsilon_F \sim 10^{-4}$, which results in Eq. (22).

[1] J. C. Slonczewski, J. Magn. Magn. Mater. **159**, L1 (1996); **195**, L261 (1999).
[2] L. Berger, Phys. Rev. B **54**, 9353 (1996).
[3] W. H. Rippard, M. R. Pufal, and T. J. Silva, Appl. Phys. Lett. **82**, 1260 (2003).
[4] I. K. Yanson, Y. G. Naidyuk, D. L. Bashlakov, V. V. Fisun, O. P. Balkashin, V. Korenivski, A. Konovalenko, and R. I. Shekhter, Phys. Rev. Lett. **95**, 186602 (2005).
[5] A. Kadigrobov, S. I. Kulinich, R. I. Shekhter, M. Jonson, and V. Korenivski, Phys. Rev. B **74**, 195307 (2006).
[6] A. M. Kadigrobov, S. Andersson, D. Radić, R. I. Shekhter, M. Jonson, and V. Korenivski, J. Appl. Phys. **107**, 123706 (2010).
[7] A. M. Kadigrobov, S. Andersson, H.-C. Park, D. Radić, R. I. Shekhter, M. Jonson, and V. Korenivski, J. Appl. Phys. **111**, 044315 (2012).
[8] J. E. Davies, O. Hellwig, E. E. Fullerton, J. S. Jiang, S. D. Bader, G. T. Zimanyi, and K. Liu, Appl. Phys. Lett. **86**, 262503 (2005).
[9] L. L. Bonilla and S. W. Teitsworth, *Nonlinear Wave Methods for Charge Transport* (Wiley-VCH, 2010).
[10] A. V. Gurevich and R. G. Mints, Rev. Mod. Phys. **59**, 941 (1987).
[11] V. V. Barelko, V. M. Beibutyan, Yu. E. Volodin, and Ya. B. Zeldovich, Sov. Phys. Doklady **26**, 335 (1981).
[12] R. Landauer, Phys. Rev. A **15**, 2117 (1977).
[13] B. Ross and J. D. Litster, Phys. Rev. A **15**, 1246 (1977).
[14] A. A. Slutskin and A. M. Kadigrobov, JETP Lett. **28**, 201 (1978).
[15] A. M. Kadigrobov, A. A. Slutskin, and I. V. Krivoshei, Sov. Phys. JETP **60**, 754 (1984).
[16] Yu. N. Chiang and I. I. Logvinov, Sov. J. Low Temp. Phys. **8**, 388 (1982).
[17] V. V. Boiko, Yu. F. Podrezov, and N. P. Klimova, JETP Lett. **35**, 649 (1982).
[18] G. I. Abramov, A. V. Gurevich, V. M. Dzugutov, R. G. Mints, and L. M. Fisher, JETP Lett. **37**, 535 (1983).
[19] A. M. Kadigrobov, Yu. N. Chiang, and I. I. Logvinov, Sov. Phys. Solid State **28**, 1903 (1986)
[20] V. N. Morgun, V. A. Bondar', A. M. Kadigrobov, and N. N. Chebotaev, Physics of the Solid State **35**, 31 (1993)
[21] V. M. Atrazhev and I. T. Yakubov, High Temp. (USSR) **18**, 14 (1980).
[22] G. I. Abramov, A. V. Gurevich, S. I. Zakharchenko, R. G. Mints, and L. M. Fisher, Sov. Phys. Solid State **27**, 1350 (1985).
[23] V. Korenivski and D. C. Worledge, Appl. Phys. Lett. **86**, 252506 (2005).
[24] An orientational phase transition in such a system induced by an external magnetic field was considered in Ref. 25.
[25] G. Asti, M. Solzi, M. Ghidini, and F. M. Neri, Phys. Rev. B **69**, 174401 (2004).
[26] S. Andersson and V. Korenivski, IEEE Trans. Magn. **46**, 2140 (2010).
[27] J. C. Slonczewski, Phys. Rev. B **39**, 6995 (1989).
[28] Typical current densities needed for the spin transfer torque effect in point-contact devices are of order 10^8–10^9 A/cm^2 when the current flows perpendicular to the layers (CPP configuration) (Ref. 29).
[29] D. C. Ralph and M. D. Stiles, J. Magn. Magn. Mater. **320**, 1190 (2008).
[30] L. D. Landau and E. M. Lifshitz, *Electrodynamics of Continuous Media* (Elsevier, Amsterdam, 2009), Sec. 26.

[31] While in general the use of periodic boundary conditions is a convenient approximation (which is excellent if $L \gg L_c$ as assumed here) they can also correctly describe the experimental situation. This is the case, e.g., in contactless experiments on ring-shaped samples. Here a slow variation of the strength of a magnetic flux that penetrates the ring can be used to generate an azimuthal electric field. Such an experiment for the observation of electrical domains in metals was suggested in Ref. 14 and experimentally realized in Ref. 16. Importantly, the necessary electric field strength is five to six orders magnitude weaker for metals than for semiconductors.

[32] Assuming a time and coordinate dependence of the form $T(x - \mathrm{st})$ and $\Theta(x - \mathrm{st})$, corresponding to a moving magnetothermoelectric domain, is a standard approach for describing moving electric domains both in semiconductors (Ref. 33) and normal metals (Ref. 10) that is justified by the temporal and spatial translation symmetry of the nonlinear partial differential equations that describe them.

[33] L. L. Bonilla and S. W. Teitsworth, *Front Matter, in Nonlinear Wave Methods for Charge Transport* (Wiley-VCH Verlag GmbH & Co. KGaA, Weinheim, Germany, 2010).

[34] A. V. Gurevich and R. G. Mints, JETP Lett. **31**, 48 (1980).